LETTERS

A large discontinuity in the mid-twentieth century in observed global-mean surface temperature

David W. J. Thompson[1], John J. Kennedy[2], John M. Wallace[3] & Phil D. Jones[4]

Data sets used to monitor the Earth's climate indicate that the surface of the Earth warmed from ~1910 to 1940, cooled slightly from ~1940 to 1970, and then warmed markedly from ~1970 onward[1]. The weak cooling apparent in the middle part of the century has been interpreted in the context of a variety of physical factors, such as atmosphere–ocean interactions and anthropogenic emissions of sulphate aerosols[2]. Here we call attention to a previously overlooked discontinuity in the record at 1945, which is a prominent feature of the cooling trend in the mid-twentieth century. The discontinuity is evident in published versions of the global-mean temperature time series[1], but stands out more clearly after the data are filtered for the effects of internal climate variability. We argue that the abrupt temperature drop of ~0.3 °C in 1945 is the apparent result of uncorrected instrumental biases in the sea surface temperature record. Corrections for the discontinuity are expected to alter the character of mid-twentieth century temperature variability but not estimates of the century-long trend in global-mean temperatures.
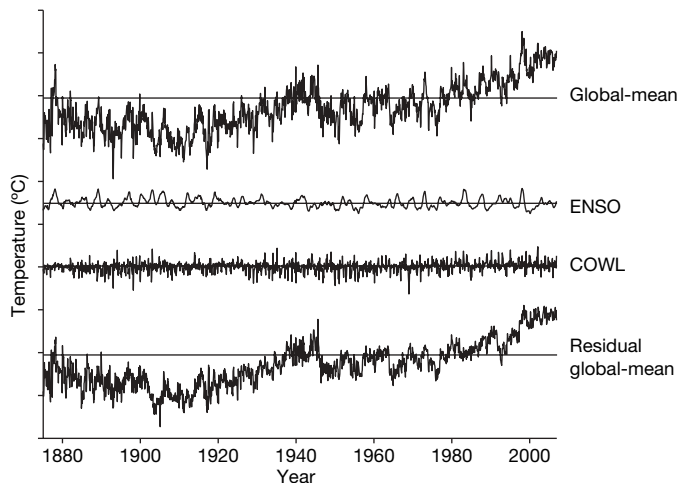
The time series of global-mean surface temperatures (T_G) reflects the influence of both anthropogenically induced and internally driven climate variability. A common method used to identify the signature of anthropogenic emissions in T_G is to compare the observed temperature variability with the output of climate change simulations. An alternative approach used to isolate the anthropogenic signal in T_G is to filter out the variance associated with internally driven climate phenomena and then interpret the residual time series. Here we exploit the latter technique to filter out the variance in T_G associated with two prominent internally driven climate phenomena: (1) the El Niño/Southern Oscillation (ENSO); and (2) temperature advection over the high latitudes of the Northern Hemisphere during winter.

The data and details of the filtering method are described in Methods. Briefly, the signal of ENSO in T_G is modelled as the damped thermodynamic response of the tropics to anomalous sea–air fluxes of sensible and latent heat in the dynamically active cold-tongue region of the eastern tropical Pacific[3]. The resulting ENSO index time series (T_{ENSO}; Fig. 1) is analogous to a lagged and low-pass-filtered time series of sea surface temperatures (SSTs) averaged over the eastern tropical Pacific, and provides a substantially better rendition of the ENSO signal in globally averaged temperatures than the more commonly used cold-tongue index (Table 1).

The signal of temperature advection over the high latitudes of the Northern Hemisphere is manifested in the so-called 'cold oceans–warm land' (COWL) pattern[4]. During months with abnormally strong westerly winds at the surface, there is enhanced advection of relatively warm marine air masses over the colder continents and cold continental air masses over the warmer oceans. The continents have a lower heat capacity than the oceans, hence the warming of the land exceeds

the cooling of the ocean, and the global-mean temperature for that month is anomalously high. Months with abnormally weak surface westerlies are marked by global-mean temperature anomalies in the opposite sense. The calculation of the COWL pattern and its associated index time series is described in Methods. The COWL index time series (T_{COWL}) accounts for a substantial amount of the month-to-month weather-related 'noise' in T_G but also has weak secular variability due in part to trends in the atmospheric circulation (Fig. 1).

The influences of ENSO and the COWL pattern on surface temperatures were removed by subtracting the linearly fitted T_{ENSO} and T_{COWL} index time series from T_G (Methods). The resulting residual global-mean temperature time series ($T_G^{residual}$) is shown at the bottom of Figs 1 and 2. Filtering out ENSO and the COWL pattern reduces substantially the amount of interannual and month-to-month variance in T_G without reducing its temporal resolution. Consequently, the residual time series provides a cleaner rendition of the interdecadal variability in the time series of twentieth-century global-mean temperatures while retaining and increasing the prominence of numerous discrete drops in it. Most of the more prominent drops that are apparent in $T_G^{residual}$ coincide with large tropical

Figure 1 | Filtering out the ENSO and COWL signatures from the global-mean temperature time series. From top to bottom: the time series of global-mean, monthly-mean surface temperature anomalies based on the HadCRUT3 combined SST and land surface air temperature data (T_G; data described in Methods); the contribution of T_{ENSO} to T_G; the contribution of T_{COWL} to T_G; the residual global-mean time series found by removing from T_G the linear contributions of T_{ENSO} and T_{COWL}. Vertical axis shows temperature anomalies; tickmarks indicate steps of 0.5 °C. Horizontal lines denote the mean of the respective time series for the 1961–90 period. The calculation of the ENSO and COWL index time series and the linear fitting technique are described in Methods.

[1]Department of Atmospheric Science, Colorado State University, Fort Collins, Colorado 80523, USA. [2]Met Office Hadley Centre, Exeter EX1 3PB, UK. [3]Department of Atmospheric Sciences, University of Washington, Seattle, Washington 98195, USA. [4]Climatic Research Unit, School of Environmental Sciences, University of East Anglia, Norwich NR4 7TJ, UK.

Table 1 | Correlations between indicated time series

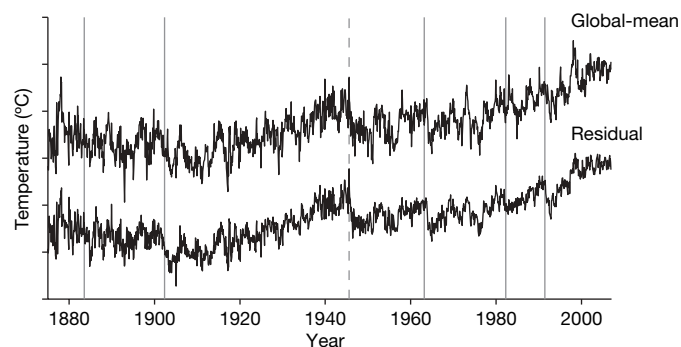|	T_G	T_G^{Land}	T_G^{Ocean}
Cold-tongue index	**0.28**	0.16	**0.39**
T_{ENSO}	**0.38**	**0.30**	**0.45**
COWL	**0.41**	**0.50**	−0.02

The cold-tongue index corresponds to SST anomalies averaged over the region 5° N–5° S and 180–90° W. The analyses used to calculate the T_{ENSO} and COWL index time series and the data used to calculate the global-mean combined land+ocean (T_G), land (T_G^{Land}) and ocean (T_G^{Ocean}) time series are described in Methods. Correlations are based on detrended monthly-mean data 1950–2006. Bold font denotes correlations that are significant at the 95% level assuming one degree of freedom per year.

volcanic eruptions (Fig. 2; solid vertical lines). However, the most pronounced drop occurs in late 1945 and is not associated with any known climate phenomenon. The signal of the volcanic eruptions in the residual data is discussed elsewhere (D.W.J.T. *et al.*, manuscript in preparation); here we focus on the discontinuity in late 1945.

The discontinuity in global-mean surface temperatures in late 1945 is evident in the unfiltered global-mean time series, but its prominence and unique character are highlighted by the removal of the ENSO and COWL-related variability (Fig. 2). The amplitude of the step is substantial: temperatures dropped by ~0.3 °C during the ~6-month period following August 1945, thus the amplitude of the drop is roughly 40% as large as the ~0.75 °C rise in T_G from 1900 to 2006, and is larger than the drop in T_G following the June 1991 eruption of Mt Pinatubo (Fig. 2 bottom time series). Clearly, the step has a profound impact on the historical record of twentieth-century surface temperatures.

The step in late 1945 does not appear to be related to any known physical phenomenon. No substantial volcanic eruptions were reported at the time, and the nuclear explosions over Hiroshima and Nagasaki are estimated to have had little effect on global-mean temperatures: ~100 Hiroshima-sized explosions are predicted to lead to a global-mean cooling of ~1.25 °C (ref. 5), thus two such explosions might be expected to lead to a cooling of less than 0.03 °C. Furthermore, ocean and land areas should both respond to an external forcing, but the step is only apparent in SSTs (Fig. 3). The global-mean land time series does not exhibit warming from the middle of the century until about 1980, but there is no large discrete drop in late 1945 in the unfiltered land series and only an indistinct drop in the residual land series (Fig. 3b). As is the case for the global-mean time series in Fig. 2, the drop is apparent in the unfiltered global-mean SST time series but is highlighted after filtering out the effects of internal climate variability.
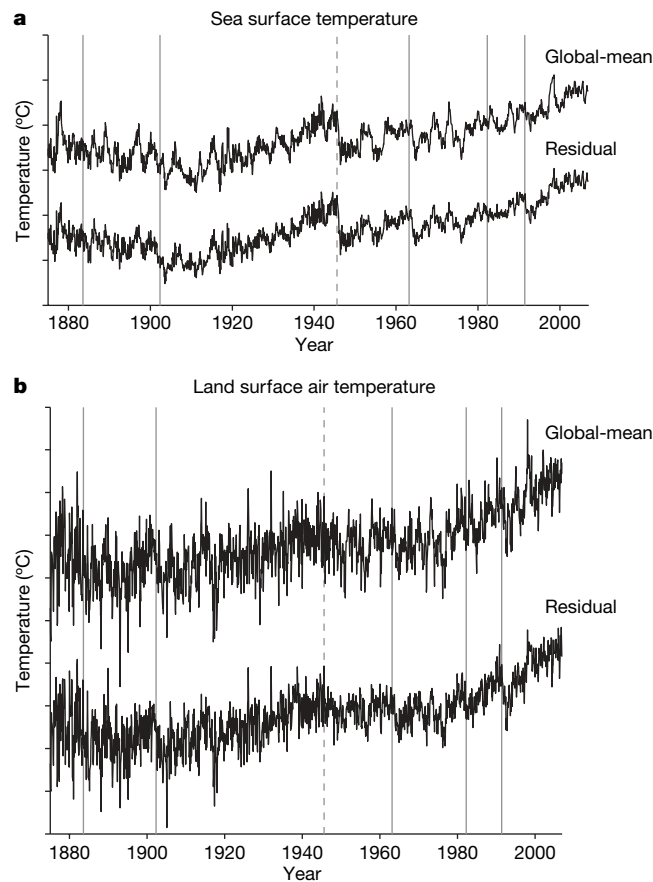
Why did global-mean SSTs drop so rapidly in late 1945? At the time, SST data were sampled on board ships using a variety of measurement techniques, including measurements taken from insulated and uninsulated buckets and engine room intakes (see refs 6–9 and

references therein). Different measurement techniques are prone to different physical biases. For example, bucket measurements are affected by the exchange of sensible, latent and radiant heat with the surrounding environment, and are often biased cool relative to the actual temperature. Engine room intake measurements are influenced by the proximity of the ship's engine and the depth of the intake water, and are most often biased warm[6,9]. The effect of changes in instrumentation on SST measurements can be corrected only with knowledge of both the physical biases and a time history of the way in which measurements were taken.

The results shown here are based on the current version of the UK Met Office Hadley Centre SST data set (HadSST2; ref. 9). Like all historical SST products, the HadSST2 data are derived from the database of raw (that is, uncorrected) marine observations provided by the International Comprehensive Ocean-Atmosphere Data Set (ICOADS; ref. 10), or one of its predecessors. The SST data in the ICOADS archive are affected by numerous changes in instrumentation. The HadSST2 data have been corrected for the widespread use of uninsulated buckets in the nineteenth and early twentieth century, and for the large change in instrumentation which occurred when US Merchant Marine ships switched from uninsulated bucket measurements to engine room intake measurements between 1939 and the end of 1941 (refs 6, 9). The corrections were made by adjusting the data before 1941 so that they are compatible with the data obtained from the mix of measurements during the 1961–90 period, and they

Figure 2 | The original (that is, unfiltered) and residual global-mean temperature time series duplicated from Fig. 1. The solid vertical lines denote volcano eruption dates: from left to right, Mts Krakatoa, Santa Maria, Agung, El Chichón and Pinatubo. The dashed vertical line denotes the month of August 1945. Vertical axis shows temperature anomalies; tickmarks indicate steps of 0.5 °C.

Figure 3 | Filtering the SST and land temperature time series. a, The original and ENSO-residual global-mean SST time series based on the HadSST2 data. **b,** The original and ENSO+COWL residual land surface temperature time series based on the CRUTEM3 land temperature data. Vertical lines are as in Fig. 2. Vertical axis shows temperature anomalies; tickmarks indicate steps of 0.5 °C in both **a** and **b**. The residual global-mean SST time series is formed by subtracting T_{ENSO} from the unfiltered SST time series (the COWL index time series is not significantly correlated with the global-mean SST time series; Table 1).
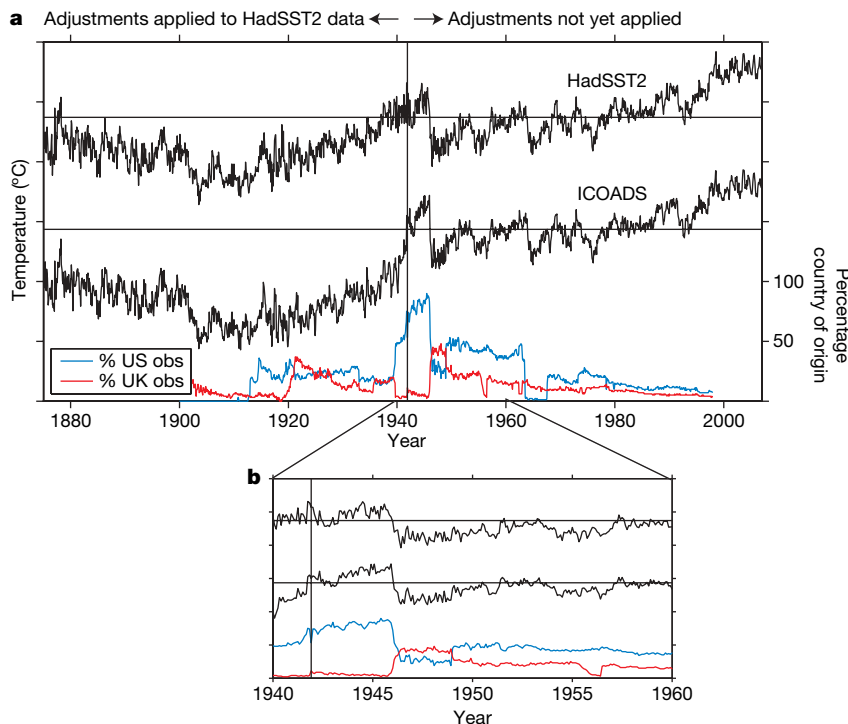
Figure 4 | The HadSST2, ICOADS and country-of-origin time series. a, Top, the ENSO residual global-mean SST time series reproduced from Fig. 3. Middle, as in the top time series but for data from ICOADS. Bottom, the percentage of observations which can be positively identified as coming from US (blue) and UK (red) ships. The vertical line denotes December 1941. Data to the left of the vertical line were corrected in the Met Office Hadley Centre data[6,9]; data to the right of the vertical line have not been adjusted in the HadSST2 data. **b,** As **a** but focused on the period 1940–60. Left vertical axis shows temperature anomalies; tickmarks indicate steps of 0.5 °C. Right vertical axis shows percentage of observations. Horizontal lines in the temperature time series denote the mean for 1961–90.

result in the large differences between the ICOADS and HadSST2 data before 1941 (Fig. 4). However, these are the only substantial corrections that have been applied to the HadSST2 data, in part because important information about the mix of measurements for the post-Second World War era has only recently been digitized[11]. From the country-of-origin information in Fig. 4, it is clear that the SST archive—and hence the mix of measurement methods—continued to evolve considerably during the decades following 1941.

The most notable change in the SST archive following December 1941 occurred in August 1945. Between January 1942 and August 1945, ~80% of the observations are from ships of US origin and ~5% are from ships of UK origin; between late 1945 and 1949 only ~30% of the observations are of US origin and about 50% are of UK origin. The change in country of origin in August 1945 is important for two reasons: first, in August 1945 US ships relied mainly on engine room intake measurements whereas UK ships used primarily uninsulated bucket measurements[12], and second, engine room intake measurements are generally biased warm relative to uninsulated bucket measurements[6,7].

Hence, the sudden drop in SSTs in late 1945 is consistent with the rapid but uncorrected change from engine room intake measurements (US ships) to uninsulated bucket measurements (UK ships) at the end of the Second World War. As the drop derives from the composition of the ICOADS data set, it is present in all records of twentieth-century climate variability that include SST data.

The Met Office Hadley Centre is currently assessing the adjustments required to compensate for the step in 1945 and subsequent changes in the SST observing network. The adjustments immediately after 1945 are expected to be as large as those made to the pre-war data (~0.3 °C; Fig. 4), and smaller adjustments are likely to be required in SSTs through at least the mid-1960s, by which time the observing fleet was relatively diverse and less susceptible to changes in the data supply from a single country of origin[9]. The new adjustments

are likely to have a substantial impact on the historical record of global-mean surface temperatures through the middle part of the twentieth century. The adjustments are unlikely to significantly affect estimates of century-long trends in global-mean temperatures, as the data before ~1940 and after the mid-1960s are not expected to require further corrections for changes from uninsulated bucket to engine room intake measurements. However, compensation for a different potential source of bias in SST data in the past decade—the transition from ship- to buoy-derived SSTs—might increase the century-long trends by raising recent SSTs as much as ~0.1 °C, as buoy-derived SSTs are biased cool relative to ship measurements[10].

METHODS SUMMARY

The data used in this study are the land-surface (CRUTEM3), sea-surface (HadSST2) and combined land- and sea-surface temperature (HadCRUT3) data obtained from the Climatic Research Unit (http://www.cru.uea.ac.uk) and described in refs 9 and 13. The methodologies used to form the ENSO and COWL index time series, and to filter out the ENSO and COWL index time series from the global-mean time series, are described in the Methods section.

Full Methods and any associated references are available in the online version of the paper at www.nature.com/nature.

1. Trenberth, K. et al. in *Climate Change 2007: The Physical Science Basis* (eds Solomon, S. et al.) Ch. 3 (Cambridge Univ. Press, Cambridge, UK, 2007).
2. Hegerl, G. et al. in *Climate Change 2007: The Physical Science Basis* (eds Solomon, S. et al.) Ch. 9 (Cambridge Univ. Press, Cambridge, UK, 2007).
3. Yulaeva, E. & Wallace, J. M. The signature of ENSO in global temperature and precipitation fields derived from the microwave sounding unit. *J. Clim.* 7, 1719–1736 (1994).
4. Wallace, J. M., Zhang, Y. & Renwick, J. A. Dynamic contribution to hemispheric mean temperature trends. *Science* 270, 780–783 (1995).
5. Robock, A. et al. Climatic consequences of regional nuclear conflicts. *Atmos. Chem. Phys.* 7, 2003–2012 (2007).

6. Folland, C. K. & Parker, D. E. Correction of instrumental biases in historical sea surface temperature data. *Q. J. R. Meteorol. Soc.* **121**, 319–367 (1995).

7. Kent, E. C. & Taylor, P. K. Toward estimating climatic trends in SST. Part I: Methods of measurement. *J. Atmos. Ocean. Technol.* **23**, 464–475 (2006).

8. Smith, T. M. & Reynolds, R. W. Bias corrections for historical sea surface temperatures based on marine air temperatures. *J. Clim.* **15**, 73–87 (2002).

9. Rayner, N. A. *et al.* Improved analyses of changes and uncertainties in sea surface temperature measured in situ since the mid-nineteenth century: The HadSST2 data set. *J. Clim.* **19**, 446–469 (2006).

10. Worley, S. J., Woodruff, S. D., Reynolds, R. W., Lubker, S. J. & Lott, N. ICOADS Release 2.1 data and products. *Int. J. Climatol.* **25**, 823–842 (2005).

11. Kent, E. C., Woodruff, S. D. & Berry, D. I. Metadata from WMO Publication No. 47 and an assessment of voluntary observing ships observation heights in ICOADS. *J. Atmos. Ocean. Technol.* **24**, 214–234 (2007).

12. *Marine Observer's Handbook* 8th edn (HMSO, London, 1963).

13. Brohan, P., Kennedy, J. J., Harris, I., Tett, S. F. B. & Jones, P. D. Uncertainty estimates in regional and global observed temperature changes: A new dataset from 1850. *J. Geophys. Res.* **111**, D12106, doi:10.1029/2005JD006548 (2006).

METHODS

All results and analyses are based on monthly-mean data. Following ref. 3, the tropical-mean surface temperature response to ENSO is modelled as:

$$C \frac{\mathrm{d}}{\mathrm{d}t} T_{\mathrm{ENSO}}(t) = F(t) - \beta T_{\mathrm{ENSO}}(t) \tag{1}$$

where $T_{\mathrm{ENSO}}(t)$ denotes the simulated response of monthly-mean tropical-mean surface temperature anomalies to ENSO variability; $F(t)$ is the anomalous flux of sensible and latent heat in the eastern tropical Pacific, parameterized as the average SST anomaly in the dynamically active cold-tongue region ($5°$ N–$5°$ S, $180°$ W–$90°$ W) multiplied by (1) the fractional area of the tropics covered by the cold-tongue region ($\sim 5\%$), and (2) a coupling coefficient of 25 W m^{-2} K^{-1}; β is a linear damping coefficient found by linearizing the Stefan–Boltzmann law, $\beta = 4\sigma T_{\mathrm{E}}^3$, where σ is the Stefan–Boltzmann constant and the mean temperature of the tropical atmosphere, T_{E}, is assumed to be ~ 255 K; C is the heat capacity of the tropics per unit area and is determined empirically such that the correlation between $T_{\mathrm{ENSO}}(t)$ and tropical-mean surface temperature anomalies is maximized (the resulting heat capacity corresponds to the entire atmosphere and the top ~ 8 m of the tropical ocean; $C = 5.2 \times 10^7$ J m^{-2} K^{-1}). The model was initialized with anomalies in the cold-tongue region starting at 1870 and the output T_{ENSO} was used from 1875 to 1995.

Following ref. 4, the COWL pattern loadings are found as:

$$\mathrm{COWL}(x) = \overline{[T(x,t) - T_{\mathrm{NH}}(t)] \cdot T_{\mathrm{NH}}(t)} \tag{2}$$

where $T(x,t)$ are Northern Hemisphere ($30°$ N–$90°$ N) temperature anomalies given as a function of space, x, and time, t; $T_{\mathrm{NH}}(t)$ denotes the time series of Northern Hemisphere ($30°$ N–$90°$ N) mean surface temperature anomalies, and the overbar denotes the time mean. The time series of the COWL pattern (T_{COWL}) is found by projecting $[T(x,t) - T_{\mathrm{NH}}(t)]$ onto $\mathrm{COWL}(x)$ at each time step.

The T_{ENSO} and T_{COWL} index time series were fitted to global-mean temperatures as:

$$x_{\mathrm{fitted}}(t) = \frac{\overline{x'(t) \cdot T_{\mathrm{G}}'(t)}}{\overline{x'^2(t)}} \cdot x(t)$$

where $x(t)$ corresponds to the monthly-mean T_{ENSO} or T_{COWL} index time series; the fractional term on the right-hand side denotes the regression of $T_{\mathrm{G}}(t)$ onto $x(t)$; and x_{fitted} corresponds to the component of $T_{\mathrm{G}}(t)$ that is linearly congruent with variations in T_{ENSO} or T_{COWL}. The regression coefficients are based on detrended values of the data so that shared trends in the time series do not contribute to the linear fits (the data are detrended for the 1950–2006 period), and are calculated for the period 1950–2006 when the data coverage is best (the results are not sensitive to reasonable changes in the period of analyses and are virtually unchanged if the data are not detrended). The regressions were done separately for T_{ENSO} and T_{COWL} as the time series are effectively uncorrelated; virtually identical results were obtained for multiple regression. In Fig. 1, the fit to the T_{ENSO} and T_{COWL} index time series was computed for global-mean combined ocean and land temperature data; in Figs 3 and 4, the fits were computed for global-mean land and ocean temperature data separately.

NEWS & VIEWS

**CLIMATE CHANGE**

Hot questions of temperature bias

Chris E. Forest and Richard W. Reynolds

An unseen measurement bias has been identified in global records of sea surface temperature. The discrepancy will need correction, but will not affect conclusions about an overall warming trend.

On page 646 of this issue, Thompson *et al.*[1] take a fresh look at the global temperature record throughout the twentieth century, which is both a central test of climate models and prima facie evidence for man-made global warming. After filtering out large-scale natural effects, they uncover a large discontinuity in the data in 1945, and trace its source to a change in the instrumental bias in the sea-surface temperature (SST) record that occurred around that time, and has not previously been adjusted. But how did this discrepancy come about? And how does it affect the credibility of the temperature record and, by extension, models of global warming in general?

In answering the first question, it is important to realize that SST and land-temperature observations are very different. The network of measuring stations on land is relatively fixed, not tending to wander in space. At a given station, thermometers are continually and reproducibly calibrated to give a continuous, benchmarked record. Changes at individual stations that might affect the measurements — if a station is moved, for example, or if the surrounding environment changes — can be corrected. Discovering additional unexpected biases in land temperatures would mean finding systematic changes in the whole observing system. Given the attention paid to these issues in, for example, the four assessment reports of the Intergovernmental Panel on Climate Change (IPCC) over the past two decades[2], as well as in the US Climate Change Science Program's final report on temperature trends in the lower atmosphere[3], it is generally accepted that such a development is highly unlikely. The records represent a best possible estimate of the changes in land-surface temperatures.

For the oceans, the situation is different. Until the 1970s, SST observations were made entirely from ships. (After 1970, temperatures were also measured using moored and drifting buoys and, from the early 1980s, using satellites.) Different ships used different measurement methods over the years, each of which potentially had different biases. Some measurements were made by lowering uninsulated buckets over the ship's side; these tend to produce colder temperatures, owing to the effects
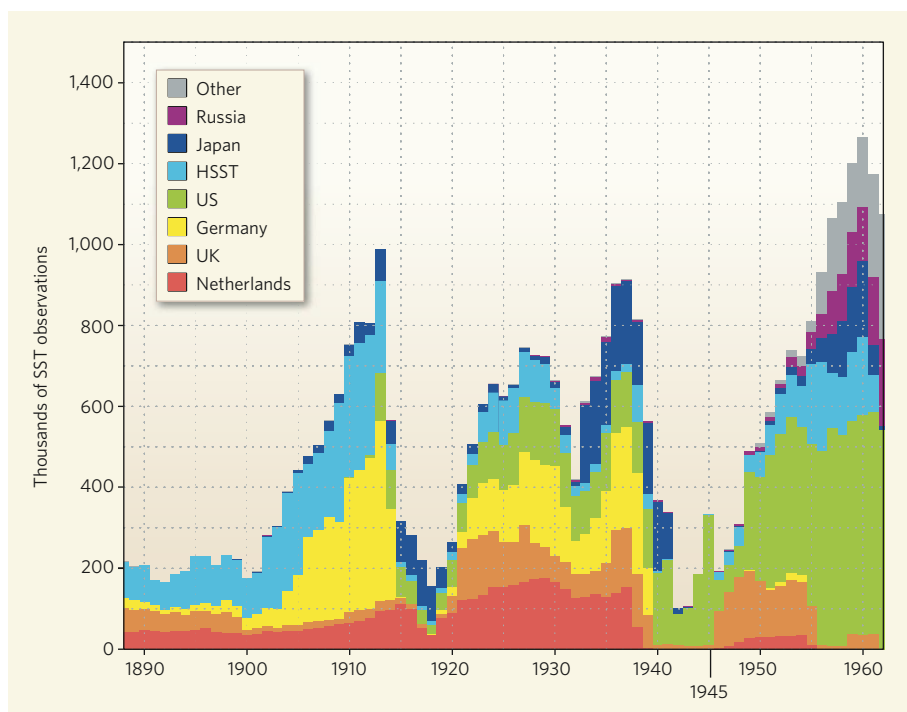
Figure 1 | Flying the flag. Sea surface temperature (SST) records from the International Comprehensive Ocean–Atmosphere Data Set[15,16], together with Historical Sea Surface Temperature (HSST) project data[17], demonstrate a wide range of national origins — and, presumably, a similar range of slightly differing measurement protocols. Thompson *et al.*[1] identify a shift in the SST record in 1945 with the resumption of a significant programme of measurement by the United Kingdom at the end of the Second World War.

of evaporation once the bucket has left the water. Other measurements were taken at the inlet for the intake of water to cool the ship's engine; these are likely to be biased towards warmer temperatures because of heating from the engine-room.

Thus, although selected SST observations can be very accurate[4,5], corrections (generally of a few tenths of a degree Celsius) can be necessary depending on how the measurements were taken. Auxiliary information — metadata — about the measurement procedure is often missing, as reporting procedures differ from country to country, and the source of the data was not always recorded. Significant corrections to the global SST record had already been undertaken in response to recognized biases: an upwards movement of the data points before

1942 was a previous attempt to account for a shift from uninsulated-bucket measurements to engine-intake measurements.

Owing to the sparseness of the metadata, Thompson *et al.*[1] use a statistical method to identify where significant biases may occur. First, because short-term variability might mask these biases, they applied a simple filter to the data to remove two sources of significant natural climate variability: the El Niño–Southern Oscillation in the Pacific, and the interplay of land and ocean temperatures in the Northern Hemisphere. What remained were two filtered time series of the global mean temperatures for land and ocean. Comparing the two, several substantial jumps can be seen, but these are mainly the aftermath of large volcanic eruptions that ejected huge amounts

of material into the stratosphere, blocking out sunlight: Krakatoa (Indonesia) in 1883, Santa Maria (Guatemala) in 1902, Agung (Indonesia) in 1963–64, El Chichón (Mexico) in 1982, and Pinatubo (Philippines) in 1991. These jumps exist in both the land and ocean data. But one shift remained a puzzle: a significant drop in SSTs from 1945 to 1946 that was not replicated in the land data. This shift is also present, but not as obvious, in the unfiltered data. In an effort to explain this change, Thompson et al. looked to the metadata — in particular, to the provenance of SST measurements from around 1945.

Figure 1 hints at the explanation; it shows the total number of SST observations from the various national temperature archives. What's striking is that both the relative fractions and the total numbers of observations vary considerably from year to year. These changes pervade the record, but unsurprisingly the two World Wars (1914–19 and 1939–45) represent the most significant shifts, both in source and in the total number of observations. And here, Thompson et al. suggest, we have the clue to the jump exposed in 1945: whereas during the preceding war years, 80% of measurements came from ships flying the US flag, a resumption of UK measurements at the end of the war saw their proportion jump to some 50%. At that time, unlike their American counterparts who took engine-intake measurements, the British relied primarily on uninsulated-bucket measurements.

So, what are the implications? Most immediately, a further correction to the global temperature series will be necessary, albeit of a magnitude yet to be assessed. There are many wider ramifications to consider, but one should be handled directly: should we doubt the rise in global mean temperatures during the twentieth century as a result of this or other hidden, and as yet undiscovered, biases in the record?

The answer is no. According to the filtering of natural variabilities that Thompson and colleagues have done, the only major discontinuity in SSTs is the one in 1945 (although other, insignificant shifts are dotted through the record). The shift from upwards-biased engine-intake measurements to downwards-biased bucket measurements demands a correction; naively speaking, temperatures between 1942 and 1945 would shift downwards by a magnitude of, say, 0.3 °C. Global warming would remain a reality — it would just be a bit more than previously thought.

How does this anticipated correction ripple through to climate models? Global mean surface temperatures are the most widely used data for evaluating the predictive capabilities of models on continental and larger scales[6–8]. They are also crucial for evaluating two other principal uncertainties in climate predictions: the factors forcing climate change (primarily, levels of aerosol particles in the atmosphere) during the twentieth century and thus in the

future[6–11]; and the rate of heat uptake from the atmosphere to the ocean (Fig. 1 in ref. 7).

The SST adjustment around 1945 is likely to have far-reaching implications for modelling in this period. One particularly striking example can be found in a figure prominently displayed on page 11 of the 18-page 'Summary for Policymakers'[12] of the IPCC's Fourth Assessment Report, produced last year. In this, the observed decadal mean temperatures of the 1940s — those that contain the anomalous 3–4 year interval dominated by (upwardly biased) US engine-room-intake measurements — are the only ones to lie above model predictions. Although we don't know exactly how the temperature record prior to 1946 will be affected by the awaited correction, it is a safe bet that temperatures in this particular decade will be lower.

The 1940s just happen to fall at the end of what seemed to be a warming trend from the 1910s that was followed by a weak decline in global temperatures into the 1960s. Climate modellers have explained the warming as a response to natural forcings[13], and the cooling as due to an increase in tropospheric aerosols, principally sulphates, as a result of increased economic activity in the decades following the Second World War. This temporarily offset the effects of man-made warming. Data analysts, on the other hand, have considered the maximum in the 1940s to be the expression of a natural fluctuation[14]. In light of the new finding[1], each interpretation will need to be reconsidered — the first of many implications that will need to be explored. ■

Chris E. Forest is in the Joint Program on the Science and Policy of Global Change, Massachusetts Institute of Technology, 77 Massachusetts Avenue, Cambridge, Massachusetts 02139, USA. Richard W. Reynolds is in the US National Climatic Data Center, National Oceanic and Atmospheric Administration, 151 Patton Avenue, Asheville, North Carolina 28801, USA.
e-mails: ceforest@mit.edu; richard.w.reynolds@noaa.gov

1. Thompson, D. W. J., Kennedy, J. J., Wallace, J. M. & Jones, P. D. Nature 453, 646–649 (2008).
2. www.ipcc.ch/ipccreports/assessments-reports.htm
3. www.climatescience.gov/Library/sap/sap1-1/default.php
4. Kent, E. C. & Taylor, P. K. J. Atmos. Ocean. Technol. 23, 464–475 (2006).
5. Kent, E. C. & Kaplan, A. J. Atmos. Ocean. Technol. 23, 487–500 (2006).
6. Forest, C. E. et al. Science 295, 113–117 (2002).
7. Stott, P. A. & Forest, C. E. Phil. Trans. R. Soc. A 365, 2029–2052 (2007).
8. Knutti, R., Stocker, T. F., Joos, F. & Plattner, G.-K. Clim. Dynam. 21, 257–272 (2003).
9. Andronova, N. G. & Schlesinger, M. E. J. Geophys. Res. 106, 22605–22612 (2001).
10. Hegerl, G. C. et al. in Climate Change 2007: The Physical Science Basis (eds Solomon, S. et al.) 663–746 (Cambridge Univ. Press, 2007).
11. Meehl, G. A. et al. in Climate Change 2007: The Physical Science Basis (eds Solomon, S. et al.) 747–846 (Cambridge Univ. Press, 2007).
12. www.ipcc.ch/pdf/assessment-report/ar4/wg1/ar4-wg1-spm.pdf (2007).
13. Stott, P. A. et al. Science 290, 2133–2137 (2000).
14. Schlesinger, M. E. & Ramankutty, N. Nature 367, 723–726 (1994).
15. Woodruff, S. D., Slutz, R. J., Jenne, R. L. & Steurer, P. M. Bull. Am. Meteorol. Soc. 68, 1239–1250 (1987).
16. Kent, E. et al. Bull. Am. Meteorol. Soc. 88, 559–564 (2007).
17. Slutz, R. J. et al. Comprehensive Ocean–Atmosphere Data Set; Release 1 (NOAA Environmental Research Laboratories, Climate Research Program, Boulder, CO, 1985).

IMMUNOLOGY

Soothing intestinal sugars

Marika C. Kullberg

The gut is a new frontier in microbiology, offering many opportunities for innovative investigation. The finding of one such study is that intestinal inflammation in mice can be tamed by bacterial sugars.

The human 'gut flora' consists of between 300 and 1,000 microbial species, and some 10^{14} microorganisms in total (about ten times the number of cells of the human body). We usually live in harmony with these microbes, and would be less healthy without them. For example, they synthesize essential vitamins and amino acids, and also degrade otherwise indigestible plant material, as well as certain drugs and pollutants.

On page 620 of this issue, Mazmanian et al.[1] report that Bacteroides fragilis, a common bacterium of the lower gastrointestinal tract in mammals, can prevent intestinal inflammation in mice. Specifically, the authors show that polysaccharide A (PSA) of B. fragilis prevents gut inflammation induced by another

bacterium, Helicobacter hepaticus, or by the chemical compound TNBS (2,4,6-trinitrobenzene sulphonic acid).

This is an exciting finding, not least given that the incidence of human intestinal inflammation and inflammatory bowel disease has increased steadily in the Western world since the early 1950s. These conditions, which include Crohn's disease and ulcerative colitis, are believed to stem in part from inappropriate immune responses to the gut microbiota[2]. In the healthy intestine, immune balance is regulated by different types of white blood cells called CD4^{+} T lymphocytes. These cells include CD4^{+} effector T lymphocytes (which help us fight pathogens by secreting various immune mediators called cytokines) and CD4^{+}